Electromagnetic Analysis of Cloaking Metamaterial Structures

Edward P. Furlani* and Alexander Baev
The Institute for Lasers, Photonics and Biophotonics, University at Buffalo
*Corresponding author: 432 Natural Sciences Complex, Buffalo, NY 14260-3000, efurlani@buffalo.edu

Abstract: We study cylindrical and spherical shell structures that have cloaking material properties proposed by Pendry *et al*. We use 2D and 3D time-harmonic analysis to study the field distribution and power flow for various arrangements of these structures. We show that the intrinsic field directing properties of these structures enable interesting and useful field manipulation including reflection, enhancement and shielding over separate spatial regions.

Keywords: cloaking, metamaterial, electromagnetic field manipulation, field focusing

1. Introduction

Recently, Pendry et al. have proposed a method for designing a media that can be used to electromagnetically "cloak" a region [1]. The cloaking properties are derived from a coordinate transformation that mathematically "squeezes" the cloaked region into a surrounding shell structure. This transformation is mapped to tensor-valued anisotropic permittivity and permeability properties. These properties apply to the shell only, which acts as an electromagnetic shield for both its interior and exterior domains. The potential to cloak a region using a custom tailored metamaterial has attracted substantial interest especially for applications such as electromagnetic shielding and stealth technology. Furthermore, the development of such media has benefited from advances made in the field of metamaterials [2-12]. In fact, a crude cloaking system has been demonstrated at microwave frequencies using artificially structured materials [13].

To date, almost all research on cloaking media has focused on the analysis of fully cloaked cylindrical and spherical regions as shown in Fig. 1 [14-18] . In this paper we use the COMSOL RF module to study the field distribution of cylindrical (2D) and spherical (3D) cloaking metamaterial structures.

2. Cylindrical Structures - 2D Analysis

Consider a cylindrical region of radius R_2 that is centered at the origin in the *x*-*y* plane. The "cloaking" coordinate transformation proposed by Pendry *et al.*, "squeezes" the entire cylindrical region $0 \le r < R_2$ into the annulus $R_1 < r < R_2$,

$$\begin{aligned} r' &= R_1 + \alpha r, \\ \theta' &= \theta, \\ z' &= z, \end{aligned} \qquad (1)$$

where $\alpha = (R_2 - R_1)/R_2$ [1].

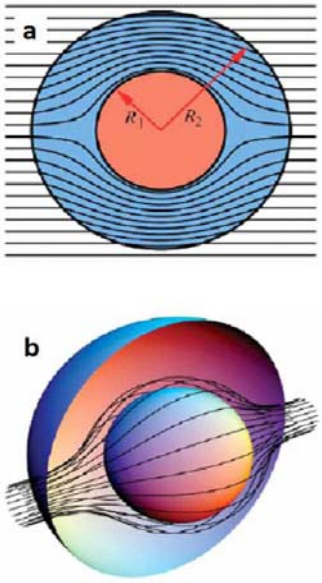

Figure1. Cloaking shells: (a) two-dimensional illustration showing bending of EM rays within a cylindrical cloaking shell, around a shielded central core, and (b) three-dimensional view of same phenomenon in a spherical geometry (adapted from [1]).

This transformation is mapped to "cloaking" material tensors $\overline{\overline{\varepsilon}}_c$ and $\overline{\overline{\mu}}_c$ as follows [16,19],

$$\bar{\bar{\varepsilon}}_c = \begin{bmatrix} \frac{r^2 + R_1(R_1-2r)\cos^2(\theta)}{r(r-R_1)} & \frac{R_1(R_1-2r)\sin(\theta)\cos(\theta)}{r(r-R_1)} & 0 \\ \frac{R_1(R_1-2r)\sin(\theta)\cos(\theta)}{r(r-R_1)} & \frac{r^2 + R_1(R_1-2r)\sin^2(\theta)}{r(r-R_1)} & 0 \\ 0 & 0 & \frac{r-R_1}{\alpha^2 r} \end{bmatrix} \quad (2)$$

Note that we have suppressed the prime notation for the transformed coordinates. Equation (2) gives the Cartesian components of the material tensors in terms of polar coordinates (r,θ), where $r = \sqrt{(x)^2 + (y)^2}$ and $\theta = \tan^{-1}(y/x)$. A similar analysis can be performed for a cloaked cylinder located anywhere in the *x*-*y* plane. Specifically, if the cylinder is centered at (x_0, y_0), we evaluate the corresponding cloaking material tensors $\bar{\bar{\varepsilon}}_c(x_0, y_0)$ and $\bar{\bar{\mu}}_c(x_0, y_0)$ by substituting

$$r(x_0, y_0) = \sqrt{(x - x_0)^2 + (y - y_0)^2},$$
$$\theta(x_0, y_0) = \tan^{-1}\left(\frac{y - y_0}{x - x_0}\right), \quad (3)$$

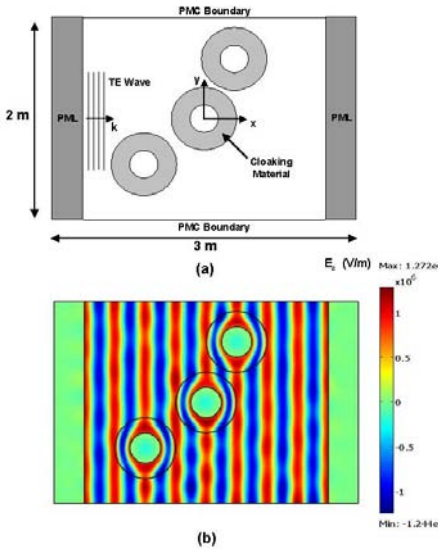

Figure 2. Three cloaked cylinders illuminated by 1 GHz TE plane wave: (a) numerical model, and (b) electric field distribution.

into Eq. (2). The cloaking material is confined to a cylindrical shell defined by

$R_1^2 \le (x - x_0)^2 + (y - y_0)^2 \le R_2^2$ and therefore

$$\bar{\bar{\varepsilon}} = \begin{cases} I & r(x_0, y_0) < R_1 \\ & r(x_0, y_0) > R_2 \\ \bar{\bar{\varepsilon}}_c(x_0, y_0) & R_1 < r(x_0, y_0) < R_2 \end{cases} \quad (4)$$

Thus, to analyze a cloaked cylinder ($r < R_1$), we solve Maxwell's equations in the x-y plane using the material properties $\bar{\bar{\varepsilon}}_c$ and $\bar{\bar{\mu}}_c$ for the cylindrical shell cloaking material, and $\bar{\bar{\varepsilon}} = \bar{\bar{\mu}} = I$ for all other regions, where *I* is the 3x3 identity matrix.

We demonstrate the theory by analyzing three separated but identical cloaked cylinders with dimensions R_1 = 0.15 m and R_2 = 0.3 m, which are centered at points (0,0), (-0.6, 0.45) and (0.3, 0.6), respectively. We perform a 2D simulation of this system using the RF solver. In the simulation, we apply Eq. (2) to each cylinder with the appropriate values of x_0 and y_0. We illuminate the cylinders with a 1 GHz transverse-electric (TE) polarized time-harmonic uniform plane wave (λ = 0.3 m) with a magnitude $E_z = 1 \times 10^6$ V/m, which is defined as the incident field in the scattered field formulation (Fig. 2a). The computational domain is 3 m long (in the direction of propagation) and 2 m high. We apply perfectly match layers (PML) at either end of the computational domain in the direction of propagation, and we impose perfect magnetic conductor (PMC) boundary conditions orthogonal to this direction (Fig. 2a). The mesh for this analysis consisted of 305,760 Lagrange cubic elements, which resulted in 1,376,941 degrees of freedom. The field solution E_z for this system, which is shown in Fig. 2b, illustrates that each cylinder is separately cloaked as expected.

Next, we study segments of cylindrical cloaking shells. We start with a single semi-shell as shown in Fig. 3a. The material properties for this geometry are as follows:

$$\overline{\overline{\varepsilon}} = \begin{cases} I & r(x_0, y_0) < R_1 \\ I & r(x_0, y_0) > R_2 \\ \overline{\overline{\varepsilon}}_c(x_0, y_0) & R_1 < r(x_0, y_0) < R_2 \\ & \frac{\pi}{2} < \theta(x_0, y_0) < \frac{3\pi}{2} \\ & R_1 < r(x_0, y_0) < R_2 \\ & -\frac{\pi}{2} < \theta(x_0, y_0) < \frac{\pi}{2} \end{cases} \quad (5)$$

where $x_0 = y_0 = 0$. We illuminate this geometry with a 1 GHz TE plane wave as above (same computational domain etc.). The analysis shows that the incident field is reflected from this structure as indicated by the peak magnitude of the field solution E_z to the left of the semi-shell as shown in Fig. 3b. The reflection at the interior surface of the shell is due to the low refractive index at $r = R_1$, i.e., the radial components of the relative permittivity and permeability are $\varepsilon_r = \mu_r = \left.\frac{r - R_1}{r}\right|_{r=a} = 0$.

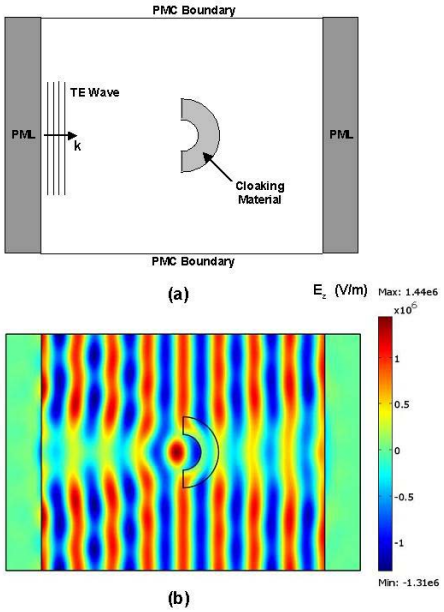

Figure 3. Semi-shell of cloaking metamaterial illuminated by 1 GHz TE plane wave: (a) numerical model, and (b) electric field distribution.

Field enhancement without reflection can be achieved using collinear semi-shells as shown in Fig. 4. We demonstrate this at an optical frequency using identical semi-shell structures with dimensions R_1 = 0.75 μm and R_2 = 1.5 μm. The semi-shells are aligned along the y-axis with their centers at $\pm R_2$, respectively. We illuminate the system with a TE plane wave with an optical wavelength λ = 532 nm. As shown in Fig. 4 (a) the field is enhanced along the x-axis to the right of the semi-shells. A normalized plot of the x-component of the time-averaged power flow is shown in Fig. 4 (b). This analysis indicates that cloaking shell segments hold potential for applications that require near- or far- field optical enhancement.

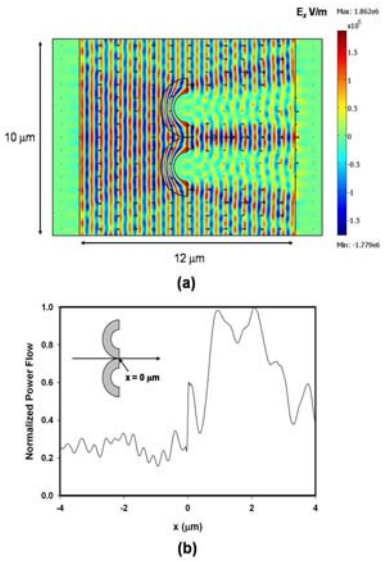

Figure 4. Optical field enhancement using collinear semi-shells: (a) E_z field distribution and time-averaged power flow vectors, and (b) normalized time-averaged x-component of the power flow along a horizontal line between the shells.

3. Spherical Structures - 3D Analysis

We now study spherical shells of cloaking metamaterial. We denote the inner and outer radii of the shell by R_1 and R_2, respectively. Following Pendry *et al.*, [1] we apply a coordinate transformation that "squeezes" the entire spherical region $0 \le r < R_2$ into the

annulus $R_1 < r < R_2$. This transformation is mapped to "cloaking" permittivity and permeability material tensors $\overline{\overline{\varepsilon}}_c = \overline{\overline{\mu}}_c$,

$$\overline{\overline{\varepsilon}}_c = \frac{R_2}{R_2\text{-}R_1}\left(\frac{r\text{-}R_1}{r}\right)^2 \hat{\mathbf{r}}\hat{\mathbf{r}} + \frac{R_2}{R_2\text{-}R_1}\hat{\boldsymbol{\theta}}\hat{\boldsymbol{\theta}} + \frac{R_2}{R_2\text{-}R_1}\hat{\boldsymbol{\phi}}\hat{\boldsymbol{\phi}} \qquad (6)$$

where $0 \le \theta \le \pi$, $0 \le \phi \le 2\pi$, and $\hat{\mathbf{r}}$, $\hat{\boldsymbol{\theta}}$, $\hat{\boldsymbol{\phi}}$ are unit vectors in spherical coordinates [1]. For the numerical analysis, we convert these material tensors to Cartesian components within the RF solver, e.g.

$$\begin{aligned}
\overline{\overline{\varepsilon}}_{c,xx} &= 1+\gamma(r)\cos^2(\phi)\sin^2(\theta) \\
\overline{\overline{\varepsilon}}_{c,xy} &= \gamma(r)\sin(\phi)\cos(\phi)\sin^2(\theta) \\
\overline{\overline{\varepsilon}}_{c,xz} &= \gamma(r)\cos(\phi)\sin(\theta)\cos(\theta) \\
\overline{\overline{\varepsilon}}_{c,yy} &= \beta(r)\sin^2(\phi)+\cos^2(\phi)-\gamma(r)\cos^2(\theta)\sin^2(\phi) \\
\overline{\overline{\varepsilon}}_{c,yz} &= \gamma(r)\sin(\phi)\sin(\theta)\cos(\theta) \\
\overline{\overline{\varepsilon}}_{c,zz} &= 1+\gamma(r)\cos^2(\theta)
\end{aligned} \qquad (7)$$

where $\beta(r) = \left(\frac{r-R_1}{r}\right)^2$ and $\gamma(r) = \beta(r) - 1$. The remaining components of the relative permittivity and permeability tensors are readily obtained from Eq. (7) as $\overline{\overline{\varepsilon}}_c$ and $\overline{\overline{\mu}}_c$, are equal and symmetric.

To analyze a cloaked sphere ($r < R_1$), we solve Maxwell's equations using the constitutive relations,

$$\overline{\overline{\varepsilon}} = \overline{\overline{\mu}} = \begin{cases} I & r < R_1 \text{ and } r > R_2 \\ \overline{\overline{\varepsilon}}_c & R_1 < r < R_2 \end{cases}, \qquad (8)$$

where I is the 3x3 identity matrix. We demonstrate the theory by modeling a cloaking shell with inner and out radii R_1 = 200 nm and R_2 = 600 nm, respectively, that is centered at the origin (Fig. 5a). The computational domain spans 5μm in the direction of propagation (z-axis), and 3 μm in both the x and y directions. We apply perfectly matched layers (PMLs) at the top and bottom of the computational domain, and impose perfect electric conductor (PEC) conditions at the boundaries perpendicular to the E field at x = ± 1.5 μm, and perfect magnetic conductor (PMC) conditions at the boundaries perpendicular to the H field at y = ± 1.5 μm. The PEC and PMC conditions ensure normal incidence of the respective fields at the boundaries transverse to the direction of propagation. Thus, they mimic a 2D array of spherical shells with a center-to-center lattice

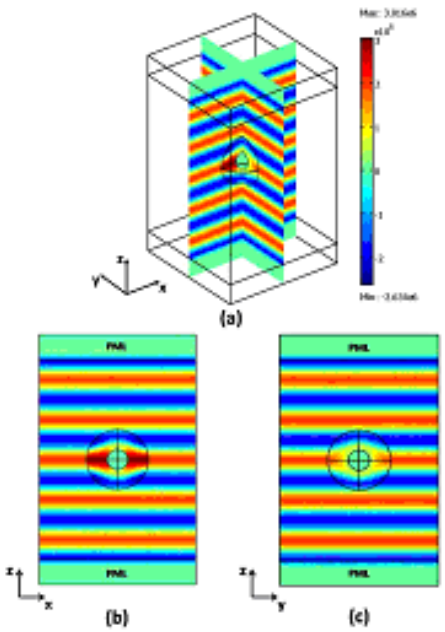

Fi

Figure 5. Full-wave time-harmonic field analysis (λ = 800 nm) of spherical shell of cloaking metamaterial: (a) E_x in two orthogonal planes showing a cloaked core ($r < R_1$), (b) E_x in the x-z plane, and (c) E_x in the y-z plane.

spacing of 3 μm in both the x and y directions. We illuminate the spherical shell with a downward directed uniform TEM plane wave with the E field along the x-axis. The incident field is generated by a time-harmonic (λ = 800 nm) surface current source positioned in the x-y plane 2 μm above the top surface of the semi-shell, i.e. at z = 2 um (immediately below the upper PML). The magnitude of the surface current is chosen to provide a plane wave with a field magnitude of $E_x = 2\times10^6$ V/m. The full-wave analysis shown in Fig. 5 demonstrates that the interior of the shell is cloaked as expected.

4. Conclusions

We have shown that the COMSOL RF solver is well suited for the analysis of cloaking metamaterial structures. We have used this program to study the field distribution of cylindrical and spherical shell metamaterial geometries. Our analysis shows that such structures can be used to control and manipulate the electromagnetic field in useful ways. If cloaking material properties can be realized in practice, then segments of this material hold potential for a broad range of applications in fields such as optics, telecommunications and nanoscale science.

5. References

[1] J. B. Pendry, D. Schurig, and D. R. Smith, "Controlling electromagnetic fields," Science **312**, 1780 (2006).

[2] J. B. Pendry, A. J. Holden, W. J. Stewart, I. Youngs, "Extremely low frequency plasmons in metallic mesostructures," Phys. Rev. Lett. **76**, 4773 (1996).

[3] J. B. Pendry, A. J. Holden, D. J. Robbins, W. J. Stewart, "Magnetism from conductors and enhanced nonlinear phenomena," IEEE Trans. Micr. Theory Techniques **47**, 2075 (1999).

[4] R. A. Shelby, D. R. Smith, S. Schultz, "Experimental verification of a negative index of refraction," Science **292**, 77 (2001).

[5] A. Houck, J. B. Brock, I. L. Chuang, "Experimental observation of a left-handed material that obeys Snell's law," Phys. Rev. Lett. **90**, 137401 (2003).

[6] Grbic, G. V. Eleftheriades, "Overcoming the diffraction limit with a planar left-handed transmission-line lens," Phys. Rev. Lett. **92**, 117403 (2004).

[7] V. M. Shalaev, W. Cai, U.K. Chettiar, H.-K. Yuan, A.K. Sarychev, V.P. Drachev, and A.V. Kildishev, "Negative index of refraction in optical metamaterials," Opt. Lett. **30**, 3356 (2005).

[8] D. R. Smith, J. B. Pendry, M. C. K. Wiltshire, "Metamaterials and negative refractive index," Science **305**, 788 (2004).

[9] E. Cubukcu, K. Aydin, E. Ozbay, S. Foteinopoulou, C. M. Soukoulis, "Electromagnetic waves: Negative refraction by photonic crystals," Nature **423**, 604 (2003).

[10] E. Cubukcu, K. Aydin, E. Ozbay, S. Foteinopolou, C. M. Soukoulis, "Subwavelength resolution in a two-dimensional photonic-crystal-based superlens," Phys. Rev. Lett. **91**, 207401 (2003).

[11] T. J. Yen, W.J. Padilla, N. Fang, D.C. Vier, D.R. Smith, J.B. Pendry, D.N. Basov, and X. Zhang, "Terahertz magnetic response from artificial materials," Science **303**, 1494 (2004).

[12] S. Linden, C. Enkrich, M. Wegener, J. Zhou, T. Koschny, and C.M. Soukoulis, "Magnetic response of metamaterials at 100 terahertz," Science **306**, 1351 (2004).

[13] D. Schurig, J. J. Mock, B. J. Justice, S. A. Cummer, J. B. Pendry, A. F. Starr, and D. R. Smith, "Metamaterial electromagnetic cloak at microwave frequencies," Science **314**, 977 (2006).

[14] F. Zolla, S. Guenneau, A. Nicolet and J. B. Pendry, "Electromagnetic analysis of cylindrical invisibility cloaks and the mirage effect," Opt. Lett. **32**, 1069 (2007).

[15] D. Schurig, J. B. Pendry, and D. R. Smith, "Calculation of material properties and ray tracing in transformation media," Opt. Express **14**, 9794 (2006).

[16] S. A. Cummer, B.-I. Popa, D. Schurig, D. R. Smith, and J. B. Pendry, "Full-wave simulations of electromagnetic cloaking structures," Phys. Rev. E **74**, 036621 (2006).

[17] H. Chen and C. T. Chan, "Transformation media that rotate electromagnetic fields," Appl. Phys. Lett. **90**, 241105 (2007).

[18] H. Chen, B-I Wu, B. Zang and J. A. Kong,, "Electromagnetic wave interactions with a metamaterials cloak," Phys. Rev. Lett. **99**, 063903 (2007).